

general applicability to other oxidation/spin states of hemoproteins.

Dynamics of Labile Proton Exchange. The exchange data reflect facile exchange of labile protons of residues buried in the highly hydrophobic interior of the protein. Such exchange is taken as direct evidence that these proteins are not static but undergo fluctuation which exposes these residues to solvent.^{22,37} We have already shown elsewhere²⁹ that the differential exchange rates of the unique proximal histidyl imidazole N₁H in deoxy myoglobin and metmyoglobin cyanide provide evidence for widely differing dynamic stabilization of the heme pocket in ligated and unligated myoglobin. Even more dramatic differences in exchange rates for peptide NH's between unligated and ligated hemoglobin have been reported based on tritium-labeling studies,²² but the location of the ligation state sensitive proton has yet to be established. Such differential amplitudes of fluctuation could serve as an allosteric control mechanism for O₂ access to and exit from the sterically blocked heme pocket in hemoglobin.

The exchange rate may be generally written³⁷

$$\tau_i^{-1} = k_A[H^+] + k_B[OH^-] + k_W[H_2O] \quad (5)$$

where k_A , k_B , and k_W are the rate constants for acid-, base-, and water-catalyzed exchange of N-H protons. The kinetic data in Figure 7 reveal that peak b exhibits only base-catalyzed exchange, i.e., $k_B \gg k_A$. Since a coordinated imidazole is not susceptible to acid attack unless the Fe-N bond is broken, the dominance of base-catalyzed exchange for the His F8 N₁H should be expected and may be diagnostic for this resonance.

On the other hand, peak a, which is due to the distal His E7 N₃H, exhibits only acid-catalyzed exchange, i.e., $k_A \gg k_B$. Bretscher had already suggested³⁸ that the N₃H of His E7 is hydrogen bonded to the coordinated cyanide. The determined $r = 4.2 \text{ \AA}$ places the proton essentially within the van der Waals contact of the coordinated cyanide, strongly supporting such an

interaction. This interaction, depicted in Figure 1, also would stabilize the proton against attack by base, which is consistent with the observed dominance of acid-catalyzed exchange. In the absence of such a strong interaction, exchange of the imidazole NH would be expected to occur by both acid and base catalysis. Such is precisely the case for peak d, assigned to His FG2. Peak c exhibits a much slower exchange rate than peaks a or b, consistent with the reduced lability of peptide protons,³⁷ which also generally feature $k_B \gg k_A$.

The slopes to the straight lines fit by a least-squares method to the data points for each resonance in Figure 7 yield slopes of 0.79 ± 0.08 for peak a, 0.77 ± 0.09 for peak b, and 0.63 ± 0.07 for peak c. There are insufficient data points to establish the slopes of either the low pH or pH sides for peak d. Thus the exchange rate is less than first order in [OH] (peak b and c) or [H⁺] (peak a), an observation which is often taken as evidence³⁷ for the EX₂ mechanism where the rate of interconversion between a buried (folded) and exposed (more random) orientation for the residue containing the exchanging proton is much faster than the rate of proton exchange with water in the exposed orientation.

Thus, our study of the dynamics of labile proton exchange demonstrates that rates can be determined over a two-decade range and that the exchange behavior with respect to pH provides not only support for some assignments for resonances determined primarily from relaxation time measurements, but also supports the presence of a strong interaction of the distal histidine with the coordinated cyanide. These exchange properties may provide additional definitive structural and/or dynamic information on myoglobin as similar data on related hemoprotein becomes available for comparison. Preliminary studies in these laboratories indicate that the exchange rates by base catalysis of the uniquely assignable proximal histidyl imidazole N₁H varies by over seven decades among such diverse hemoproteins as cytochromes *c* and *c'*, legume hemoglobin, and horseradish peroxidase.³⁶

Acknowledgment. This research was supported by a grant from the National Science Foundation (CHE-77-26517), the UCD NMR Facility, and (in part) the National Institutes of Health (HL-16087).

(36) La Mar, G. N.; de Ropp, J. S.; Kong, S. B.; Cutnell, J. D.; Jackson, J. T., to be published.

(37) Woodward, C. K.; Hilton, B. D. *Annu. Rev. Biophys. Bioeng.* 1979, 8, 88-127.

(38) Bretscher, P. A. Ph.D. Thesis, Cambridge University, England, 1968.

Communications to the Editor

Versatility of Mo(*t*-BuS)₄. Selective Formation of a Series of Thiolatomolybdenum(I), -molybdenum(II), and -molybdenum(IV) Compounds

Masato Kamata, Toshikatsu Yoshida, and Sei Otsuka*

Department of Chemistry, Faculty of Engineering Science
Osaka University, Toyonaka, Osaka 560, Japan

Ken Hirotsu and Taiichi Higuchi*

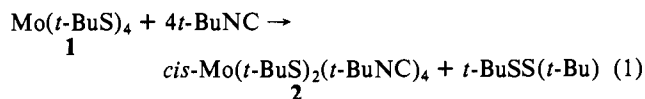
Department of Chemistry, Osaka City University
Sumiyoshiku, Osaka 558, Japan

Received February 12, 1981

Despite considerable current interest in thiolatomolybdenum compounds due to their possible implication in redox-active molybdoenzymes,^{1,2} substitution active molybdenum compounds ligated with unidentate thiolate remain rare. Recently we were

able to prepare a novel homoleptic compound, Mo(*t*-BuS)₄ (**1**).³ This compound exhibits remarkable reactivity toward various reagents ranging from nucleophiles to electrophiles. Here we wish to report the reactions with CO, *t*-BuNC, and PMe₂Ph,⁴ typical biphilic reagents varying in electronic properties.

To a stirring solution of **1** (3.5 mmol) in *n*-hexane (45 mL) was added *t*-BuNC (16.5 mmol) at ambient temperature. The initial red solution rapidly turned dark green. The solution was allowed to stand for 1 h during which time a dark green crystalline product precipitated. The mixture being cooled below -10 °C, the precipitate was collected by filtration and washed with cold *n*-hexane to remove *t*-BuSS(*t*-Bu) and unreacted *t*-BuNC. The solid product, which was found to be Mo(*t*-BuS)₂(*t*-BuNC)₄ (**2**) (85% yield), thus obtained is pure enough for further chemical trans-



(3) Otsuka, S.; Kamata, M.; Hirotsu, K.; Higuchi, T. *J. Am. Chem. Soc.* 1981, 103, 3011.

(4) All reactions are described here (except the reaction under a CO pressure) were carried out under a pure nitrogen atmosphere employing dry deaerated solvents.

(1) Reviews: (a) Stiefel, E. I. *Progr. Inorg. Chem.* 1977, 22, 1. (b) Kuehn, C. G.; Isied, S. S. *Ibid.* 1980, 27, 153-221.

(2) Newton, W. E., Otsuka, S., Eds. "Molybdenum Chemistry of Biological Significance"; Plenum Press: New York, 1980.

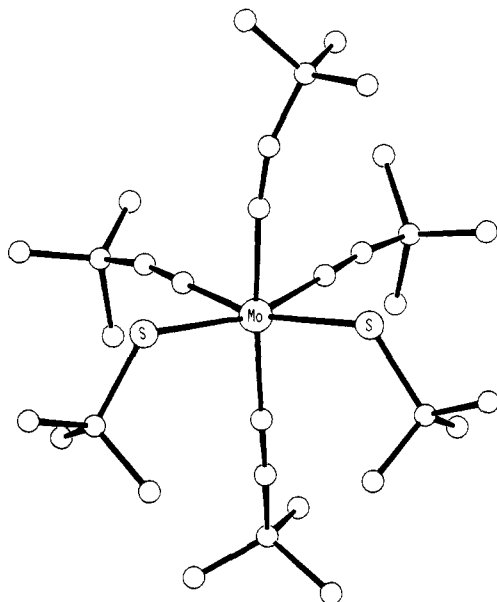


Figure 1. Molecular Structure of $\text{Mo}(t\text{-BuS})_2(t\text{-BuNC})_4$ (2).

formation. An analytically pure deep-yellow-green crystal,⁵ mp 160–161 °C, can be obtained by recrystallization from a toluene-*n*-hexane mixture. Notably, even under forcing conditions (at 100 °C with a large excess *t*-BuNC), **2** was the main product, no further reductive elimination of *t*-BuS ligands being observed. Similarly from a toluene solution of **2** and free *t*-BuNC (1:4 mol ratio) which was heated at 100 °C for 10 h, **2** was recovered without substantial loss.

The electronic spectrum (in *n*-hexane) is characterized by several strong CT absorptions at 297 (log ϵ , 4.48), 425 (3.78), 450 (sh, 3.68), and 690 nm (2.83). The *n*-hexane solution IR shows ν (N≡C) bands at 2120 and 2010 cm^{-1} , which are lower compared with the values (2138–2157 cm^{-1}) found for $\text{Mo}(\text{RNC})_7^{2+}$ (R = *t*-Bu, CH_3),⁶ reflecting the electron donation from the thiolate ligands. The ¹H NMR (C_6D_6) at ambient temperature shows two singlets at δ 1.23 (*t*-BuNC) and 1.98 (*t*-BuS) with an intensity ratio of 2:1. The ¹³C NMR (C_6D_6) at ambient temperature reveals two inequivalent *t*-BuNC ligands, δ 30.8, 31.4 (CH_3C); 54.8, 57.4 (CH_2C); 174.8, 189.6 ($\text{C}\equiv\text{N}$).

X-ray diffraction studies of **2** have shown a deformed octahedron.⁷ The structural results are shown in Figure 1. The geometry of the first coordination sphere MoS_2C_4 has approximate C_{2v} symmetry. Most conspicuously the SMoS angle is very large (115.3°), and accordingly the equatorial CMoC angle (73.7°) is much smaller than 90°. This feature is not caused by steric bulk of the *tert*-butyl groups. Deformed octahedra have been observed previously for Mo(II) and W(II) compounds^{8,9} and discussed on the basis of molecular orbital theories.¹⁰ A brief explanation for the wide SMoS angle of **2**¹¹ is that the repulsive

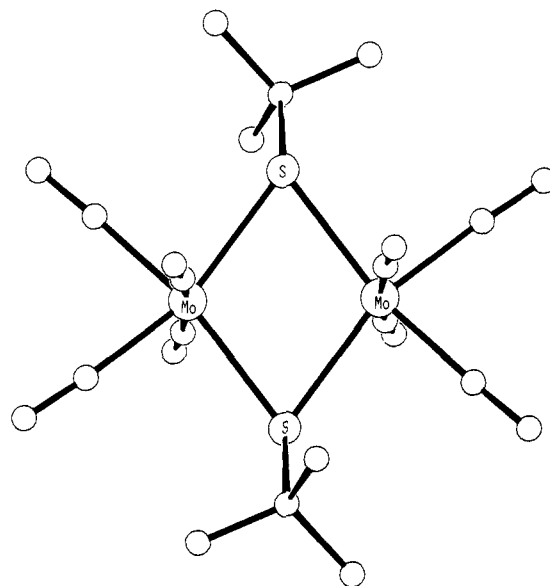
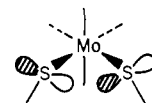


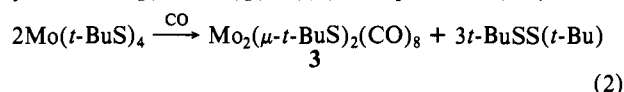
Figure 2. Molecular Structure of $\text{Mo}_2(\mu\text{-}t\text{-BuS})_2(\text{CO})_8$ (3).

interaction of the sulfur 3p lone pairs, which lie approximately in the equatorial plane, is involved in one of the occupied frontier orbitals¹² of **2**.



Compared with the number of dithioacid or dithiolato-molybdenum complexes,¹³ Mo(II) compounds of unidentate thiolates are extremely rare, only $\text{Mo}(\text{SR})_2(\text{dpe})_2$ (dpe = $\text{Ph}_2\text{PCH}_2\text{CH}_2\text{PPh}_2$)¹⁴ being reported. The Mo(II) ion with isocyanide or CO ligands has a strong propensity to assume seven-coordination,¹ thus achieving the inert gas configuration. We expect high reactivity for **2** because of its coordinative unsaturation.

The reaction of **1** with CO leads to a binuclear Mo(I) compound. Thus, a solution of freshly prepared **1** (1.0 mmol) dissolved in toluene (20 mL) was stirred under a CO atmosphere (10 kg/cm²) at ambient temperature for 10 h in a stainless steel autoclave. After purging of CO the resulting dark-green solution was evaporated to dryness to remove the solvent and a small amount of volatile byproduct, $\text{Mo}(\text{CO})_6$. The dark colored residue was recrystallized from toluene to give olive black, diamagnetic crystals of $\text{Mo}_2(\mu\text{-}t\text{-BuS})_2(\text{CO})_8$ (**3**),⁵ mp 145 °C (dec) in 67%



yield; λ_{max} (*n*-hexane) nm (log ϵ) 254 sh (4.47), 286 (4.33), 316 sh (4.08), and 656 (2.90); IR (*n*-hexane) ν (CO) 2055 (w), 1980 (s), and 1970 (s); ¹H NMR (C_6D_6) δ 1.33; ¹³C NMR δ 34.2 (CH_3C), 55.4 (CH_2C), 197.8 (CO), and 217.0 (CO). This is again a new compound; a closely related compound may be $(\text{dpe})_2\text{Mo}(\mu\text{-}n\text{-BuS})_2\text{Mo}(\text{CO})_4$.¹³ The formation of molybdenum compounds of oxidation states two or higher was not observed, reflecting the powerful ability of CO to stabilize low-valent states of transition metals.

The molecular structure of **3** was determined by X-ray crystallography.¹⁵ As shown in Figure 2, **3** is centrosymmetric. The

(5) Elemental analyses (C, H, and N) conform reasonably with theoretical values.

(6) Novotny, M.; Lippard, S. J. *J. Chem. Soc., Chem. Commun.* **1973**, 202–204.

(7) Single crystals of **2** were grown from toluene containing *n*-hexane (1:0.2 vol ratio). They belong to space group $P2_1/c$ with $a = 18.616$ (7), $b = 11.823$ (2), $c = 18.667$ (6) Å; $\beta = 116.00$ (3)°; V (for $Z = 4$) = 3693 (2) Å³; $d_c = 1.09$ g cm⁻³. $R = 6.9\%$ for 3355 reflections with $I > 3\sigma(I)$.

(8) For example, $\text{MoX}_2\text{L}_2\text{L}'_2$ (X = monobasic anion such as Br⁻, RO⁻; L, L' = neutral ligands such as pyridine, CO, PR₃).⁹

(9) (a) Chisholm, M. H.; Huffman, J. C.; Kelly, R. L. *J. Am. Chem. Soc.* **1979**, *101*, 7615–7617. (b) Templeton, J. L.; Ward, B. C. *J. Am. Chem. Soc.* **1980**, *102*, 6568–6569.

(10) Kubaček, P.; Hoffmann, R. *J. Am. Chem. Soc.*, in press.

(11) Kamata, M.; Hirotsu, K.; Higuchi, T.; Tatsumi, K.; Hoffmann, R.; Otsuka, S., in press.

(12) An out-of-phase combination of sulfur 3p orbitals is involved in the occupied frontier orbital in case of d⁴ configuration whereas this situation does not occur for d⁶ configuration.¹¹

(13) Concovanis, D. *Progr. Inorg. Chem.* **1979**, *26*, 302–469.

(14) Chatt, J.; Lloyd, J. P.; Richards, R. L. *J. Chem. Soc., Dalton Trans.* **1976**, 565–568.

(15) Single crystals of **3** were grown from toluene. They belong to $P2_1/n$ with $a = 11.998$ (10), $b = 11.229$ (5), $c = 8.856$ (6) Å; $\beta = 110.86$ (5)°, V (for $Z = 2$) = 1115 (1) Å³. $R = 4.3\%$ for 1159 reflections with $I > 3\sigma(I)$.

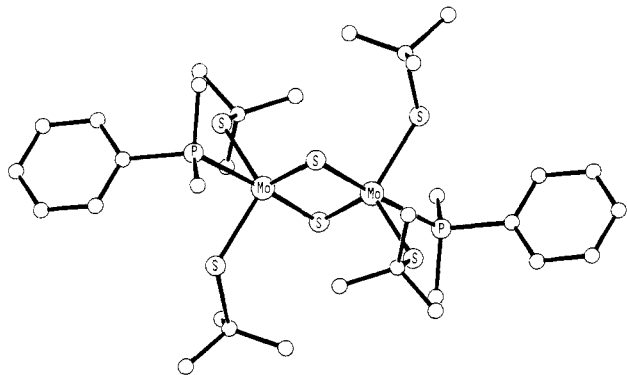
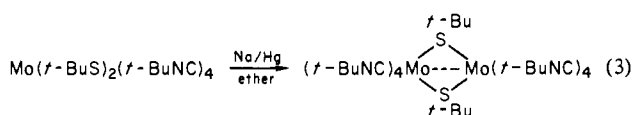


Figure 3. Molecular Structure of $\text{Mo}_2(\mu\text{-S})_2(t\text{-BuS})_4(\text{PMe}_2\text{Ph})_2$ (**5**).

geometry around Mo(I) is distorted octahedral with a large SMOs angle of $106.1(2)^\circ$ and a small equatorial CMOc angle of $81.4(5)^\circ$. The average Mo-C(equatorial) distance (2.01 \AA) is slightly shorter than the Mo-C(axial) distance (2.05 \AA). The Mo-Mo bond [$2.984(2) \text{ \AA}$] and Mo-S bond distance (2.48) are comparable to the corresponding parameters [$2.923(1)$ and 2.40 \AA] of a related compound, $\text{Mo}_2(\mu\text{-EtS})_2(\eta\text{-C}_6\text{H}_5)_2(\text{NO})_2$.¹⁶

An alkylisocyanide analogue of **3**, i.e., $\text{Mo}_2(\mu\text{-}t\text{-BuS})_2(t\text{-BuNC})_8$ (**4**),⁵ was obtained from **2**. Thus, a green solution of **2** in ether was stirred with Na/Hg at ambient temperature for 2 h.⁴ The solution turned to yellowish brown. After removing precipitated *t*-BuSNa by filtration, the solution was concentrated partially to give an analytically pure, dark brown diamagnetic crystal of **4** (75% yield), mp $165\text{--}167^\circ$ (dec); IR (*n*-hexane) $\nu(\text{N}\equiv\text{C})$ 2080



(sh), 2000 (vs), 1855 (s) cm^{-1} ; $^1\text{H NMR}$ (toluene- d_6) δ 1.30, and 1.56 (*t*-BuNC), 1.82 (*t*-BuS); λ_{max} (toluene) nm (log ϵ) 395 sh (3.59), 480 sh (3.23), 980 sh (2.45). The observation of two singlet $^1\text{H NMR}$ signals for *t*-BuNC ligands and one for *t*-BuS ligands and the IR data are consistent with a *t*-BuS bridged dimeric structure¹⁷ similar to **3**.

The observed low $\nu(\text{N}\equiv\text{C})$ frequencies compared to those found in $\text{Mo}_2(\mu\text{-Cl})_2(t\text{-BuNC})_8$ ($2146, 2123 \text{ cm}^{-1}$)¹⁸ again reflect the strong electron-donating property of the thiolate ligand. Further reduction of **4** beyond Mo(I) does not occur by prolonged contact with Na/Hg (24 h). The selective one-electron chemical reduction is amazing.

The reaction of **1** with PMe_2Ph occurs above 50°C , yielding a Mo(IV) dimeric compound. Thus a toluene solution (20 mL) containing **1** (1.0 mmol) and PMe_2Ph (2.0 mmol) was stirred⁴ at 60°C for 5 h. The initially red solution gradually turned very dark colored and finally dark green. In the vapor and liquid phase of the flask, isobutene and *t*-BuSH were detected, respectively, by GLC. The resulting reaction mixture was evaporated to dryness by vacuum distillation, and the residue was recrystallized to give a myrtle green, diamagnetic crystal of $\text{Mo}_2(\mu\text{-S})_2(t\text{-BuS})_4(\text{PMe}_2\text{Ph})_2\text{-C}_6\text{H}_5\text{CH}_3$ (**5**),⁵ mp 180°C (dec), in 80% yield; λ_{max}

$$2\text{Mo}(t\text{-BuS})_4 + 2\text{PMe}_2\text{Ph} \rightarrow \text{Mo}_2(\mu\text{-S})_2(t\text{-BuS})_4(\text{PMe}_2\text{Ph})_2 + 2(\text{CH}_3)_2\text{C}=\text{CH}_2 + 2t\text{-BuSH} \quad (4)$$

(*n*-hexane), nm (log ϵ) 290 (4.49), 329 sh (4.19), 369 (4.01), 425 sh (3.64), 446 (3.11), and 710 (3.65); IR (Nujol) 1153 cm^{-1} $\delta(\text{C}(\text{CH}_3)_3)$. The $^1\text{H NMR}$ (C_6D_6 at ambient temperature) shows a multiplet centered at δ 2.66 characteristic of an $X_6AA'X'_6$ ($|J_{AA'}| > |J_{AX} - J_{AX'}|$) spin system for the methyl protons of PMe_2Ph ,

suggesting a strong metal-metal interaction and a singlet at δ 1.16 for the *t*-BuS protons.

The molecular structure of **5** was determined by X-ray studies¹⁹ and is centrosymmetric (Figure 3). The geometry around Mo(IV) ion is best described as a distorted trigonal bipyramid with the axial phosphine and sulfide ligands. The average Mo-S(*t*-Bu) distance of 2.31 \AA is longer than that of **1**.³ The Mo-Mo distance of $2.741(1) \text{ \AA}$ is consistent with metal-metal bonding.

The formation of this sulfide-bridged dimer indicates facile dealkylation of the *t*-BuS⁻ ligand. Apparently the strong electron-donating property of PMe_2Ph is responsible for the preferential formation of Mo(IV) rather than the lower valent ions. PPh_3 reacts with **1** (60°C , 5 h), resulting in a mixture of products we have not identified yet.

Preparative applications of **1** are of course not limited to the four reactions so far described in this paper. For example, it may be useful as a molybdenum component to synthesize Mo-Fe-S mixed clusters.²⁰ Thus **1** is a versatile starting material offering a rich thiolatomolybdenum chemistry.

Acknowledgment. We thank the Ministry of Education, Japanese Government (Project No. 510207), and the Japan Synthetic Rubber Co. Ltd. for financial support and Y. Terawaki for NMR measurements. We are indebted also to the Computer Center of Osaka City University and the Crystallographic Research Center, Institute for Protein Research, Osaka University, for computer calculations.

(19) Single crystals of **5** were grown from toluene. They belong to $P\bar{1}$ with $a = 13.331(8)$, $b = 10.343(5)$, $c = 9.553(5) \text{ \AA}$; $\alpha = 97.58(4)$, $\beta = 108.62(4)$, $\gamma = 98.57(4)^\circ$; V (for $Z = 2$) = $1211(1) \text{ \AA}^3$. $R = 4.1\%$ for 2681 reflections with $I > 3\sigma(I)$.

(20) Otsuka, S.; Kamata, M., ref 2, pp 229-238.

Photochemistry of Stilbene-Capped Cyclodextrins. Exclusive Ring Closure of Cis Cap and Direct Evidence for Trans A,D Structure

Iwao Tabushi* and Lung Chi Yuan

Department of Synthetic Chemistry, Kyoto University
Yoshida, Kyoto 606, Japan
Received January 16, 1980

Since the first member of rigidly capped cyclodextrin family appeared,¹ these compounds have been gradually recognized as important key intermediates for di- (poly-) functional catalysts of various enzyme activities.² Problems of less regioselective capping by the original diphenylmethane cap elegantly displayed by Breslow^{2b} have been solved by the recent discovery of regioselective A,C- and A,D-capping reagents, benzophenone-3,3'-disulfonyl chloride and stilbene-4,4'-disulfonyl chloride,³ respectively (see Figure 1). Now we wish to report the unique photochemistry of *trans*- and *cis*-stilbene-4,4'-disulfonyl-capped β -cyclodextrins.

This photochemistry originates in our finding very efficient energy transfer between benzophenone-capped β -cyclodextrin and an appropriate naphthalene derivative;⁴ further investigations of modified cyclodextrins have been extensively pursued, such as the

(1) (a) Tabushi, I.; Shimokawa, K.; Shimizu, N.; Shirakata, H.; Fujita, K. *J. Am. Chem. Soc.* **1976**, *98*, 7855. (b) Tabushi, I.; Shimokawa, K.; Fujita, K. *Tetrahedron Lett.* **1977**, 1527-1530.

(2) (a) Tabushi, I.; Kuroda, Y.; Mochizuki, A. *J. Am. Chem. Soc.* **1980**, *102*, 1152-1153. (b) Breslow, R.; Doherty, J. B.; Guillot, G.; Hersh, C. L. *Ibid.* **1978**, *100*, 3227-3229. (c) Breslow, R.; Bovy, P.; Hersh, C. L. *Ibid.* **1980**, *102*, 2115-2117.

(3) Tabushi, I.; Kuroda, Y.; Yokota, K.; Yuan, L. C. *J. Am. Chem. Soc.* **1981**, *103*, 711-712.

(4) Tabushi, I.; Fujita, K.; Yuan, L. C. *Tetrahedron Lett.* **1977**, 2503-2506.

(16) Clark, G. R.; Hall, D.; Marsden, K. *J. Organometall. Chem.*, **1979**, *177*, 411-434.

(17) An X-ray crystallographic analysis of **4** has been undertaken.

(18) King, R. B.; Saran, M. S. *Inorg. Chem.* **1974**, *13*, 2453-2457.